

# 다해상도 웨이블릿 분해와 웨이블릿 부밴드의 에지 특성을 이용한 차량 번호판 추출에 관한 연구

정희원 박성욱\*, 황수철\*\*, 박종욱\*

## A Study on the Vehicle Plate Extraction Using Multiresolution Wavelet Decomposition and Edge Properties of Wavelet Subband

Sung-Wook Park\*, Su-Cheol Hwang\*\*, Jong-Wook Park\* *Regular Members*

### 요약

차량 번호판 자동 인식 시스템에서 번호판 영역 추출은 전체 시스템의 인식률에 가장 큰 영향을 주는 중요한 부분이다. 본 논문에서는 다해상도 웨이블릿 분해와 웨이블릿 부밴드의 에지 특성을 이용한 번호판 영역을 추출하는 방법을 제안한다. 웨이블릿으로 분해된 영상의 고주파 부대역에는 수평, 수직, 그리고 대각 방향의 에지 정보를 가지고 있으며, 차량 영상의 헤드라이트 라디에이터 헤드라이트 영역과 번호판 영역은 다른 영역에 비해서 각 방향의 에지가 집중적으로 분포한다. 본 논문에서는 이러한 에지 특성을 이용한 번호판 영역 추출 방법을 보였으며, 다양한 차량 영상을 이용하여 제안한 방법을 실험하였다. 그 결과 기존의 방법들이 가지고 있는 문제점들을 해결할 수 있었고 높은 정확성을 나타내었다.

### ABSTRACT

License plate region extraction which affects recognition rate of whole system significantly is the most important part in automatic vehicle license plate recognition system. In this paper, we propose a method to extract the license plate region using multiresolution wavelet decomposition and edge properties of wavelet subband. The High Frequency Subband(HFS) of an image, which is decomposed by wavelet, has edge information for horizontal, vertical and diagonal direction. Edge information is concentrated in each direction of the Headlight-Radiator-Headlight(H-R-H) and the license plate region compared to other regions in the vehicle image. This paper shows a license plate region extraction method using these edge properties and our experimental results with various vehicle images. In our experiments, we tested the proposed method against existing methods and we achieved high accurate results in comparison.

### 1. Introduction

Computer vision based Automatic Vehicle Identification System(AVIS) can be applied to identify speeding vehicles, stolen cars, used in automatic toll payment on highways, bridges or tunnels, and automatic parking systems etc.<sup>[1]</sup>. Vehicle license plate automatic recognition technology for AVIS

consists of 5 major parts. They are, vehicle detection, image acquisition, license plate region extraction, individual character extraction and recognition, and data transmission. Among them, license plate region extraction is most important in that it affects the overall successful recognition rate more than any other part. But, it is not easy to extract the license plate region from a vehicle

\* 인천대학교 전자공학과 시각시스템연구실(psw@incheon.ac.kr),  
논문번호 : 020077-0219, 접수일자 : 2002년 2월 19일

\*\* 인하공업전문대학 컴퓨터정보공학부(schwang@ture.inhatc.ac.kr)

image for many reasons. The quality of vehicle image, varying surroundings, different vehicle structure and types, and the color of the license plate after it is acquired by image acquisition, varies according to weather conditions<sup>[2]</sup>.

The major conventional methods for the plate region extraction can be divided into 3 classes, which are Feature Based, Gray-level Intensity Based and Color Based. The Feature Based method extracts the edge of the image and detects horizontal and vertical edge of a license plate border using the Hough Transform(HT). This method is based on the facts that the license plate of a vehicle is rectangular, the width to height ratio is 2 to 1, and is robust to noise. This method, however, is very sensitive to plate border deformation and it can fail to recognize the plate. The HT also needs much processing time. The Gray-level Intensity Based method extracts the plate region using the regular difference of gray-level intensity. It is hard to extract plate region with this method, because gray-level intensity is sensitive to environmental variation and there are many gray-level intensity parts similar to the plate region on a vehicle. The Color Based method uses the color information of the plate region. However, if the vehicle body color is similar to the plate color, plate extraction is difficult<sup>[3][4]</sup>.

In this paper, we propose a method of the plate region extraction using the edge properties of wavelet subband. First, we decompose the vehicle image by wavelet and calculate the average of HFS coefficients in each subband. We then calculate the correlation coefficient between the average of coefficients and coefficients of each HFS. From the result we can extract a region that has the maximum correlation coefficient value as a plate region. An overview of the plate region extraction is shown in Fig. 1.

This paper is organized as follows. In Section 2, we describe the wavelet decomposition for a plate region extraction. In Section 3, we present the plate region extraction method. Section 4 is to show experimental results. The conclusion and

future works are described in Section 5.

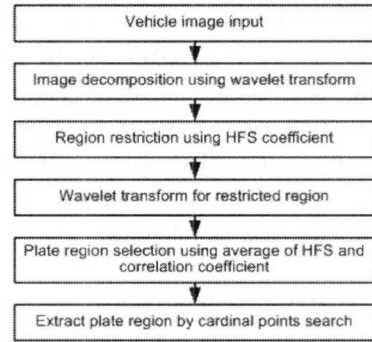


Fig. 1 Overview of the plate region extraction

## II. Wavelet Decomposition for Plate Region Extraction

### 2.1 Wavelet Decomposition

Wavelet Transform (WT) based approaches are becoming increasingly popular in texture analysis, pattern recognition and character recognition<sup>[5]</sup>. The basic functions of WT are obtained by dilating and translating a mother wavelet  $\varphi(t)$  with variable  $a$  and  $b$  in time axis. The Continuous Wavelet Transform of a 1-D signal  $f(t)$  is defined as

$$W_f(a, b) = \int_{-\infty}^{+\infty} \varphi_{a,b}(t) f(t) dt \quad (1)$$

where the wavelet  $\varphi_{a,b}$  is computed from the mother wavelet  $\varphi$  by translation and dilation.

$$\varphi_{a,b}(t) = \frac{1}{\sqrt{a}} \varphi\left(\frac{t-b}{a}\right) \text{ where } a \in R^+, b \in R, a \neq 0 \quad (2)$$

$R^+$  and  $R$  are positive real numbers and real number respectively. In case of Discrete Wavelet Transform (DWT), the parameters  $a, b$  of Eq. 2 have discrete integer values.

$$a = a_0^m, b = nb_0 a_0^m \text{ with } (m, n) \in Z, \text{ and } a_0 > 1, b_0 > 0 \quad (3)$$

In Eq. 3,  $m$  and  $n$  are integer parameters related to scale and time-shift, respectively. Therefore, mother wavelet  $\varphi$  is

$$\varphi_{m,n}(t) = a_0^{-m/2} \varphi(a_0^{-m} t - nb_0) \quad (4)$$

In Eq. 4, in the case of  $a_0=2$  and  $b_0=1$ , there is a very special choice for  $\varphi$ , such as  $\varphi_{m,n}$  which constitutes an orthogonal basis (dyadic decomposition). In this case, the DWT can be performed efficiently using Quadrature Mirror Filters (QMF) [6]. Each QMF pair consists of low-pass ( $H$ ) and high-pass filters ( $G$ ), which splits a signals' bandwidth in half. 2-D DWT is computed by applying separable filter bank as following:

$$\begin{aligned}
 L_n(b) &= [H_x * [H_y * L_{n-1}]_{\downarrow 2,1}]_{\downarrow 1,2}(b) \\
 D_{n1}(b) &= [H_x * [G_y * L_{n-1}]_{\downarrow 2,1}]_{\downarrow 1,2}(b) \\
 D_{n2}(b) &= [G_x * [H_y * L_{n-1}]_{\downarrow 2,1}]_{\downarrow 1,2}(b) \\
 D_{n3}(b) &= [G_x * [G_y * L_{n-1}]_{\downarrow 2,1}]_{\downarrow 1,2}(b), \text{ with } b \in R^2
 \end{aligned}
 \tag{5}$$

where  $R^2$  denotes two dimensional Euclidean space,  $*$  is the convolution operator, and  $\downarrow 2,1(\downarrow 1,2)$  denotes subsampling along rows(columns).  $H$  and  $G$  are low-pass and high-pass filter respectively.  $L_n$  is obtained by LPF and is referred to as low resolution image at scale  $n$ .  $D_{ni}$  is referred to as detail images at scale  $n$  and contains detailed information of horizontal( $D_{n1}$ ), vertical( $D_{n2}$ ) and diagonal( $D_{n3}$ ) directions; which is obtained from the HPF. Therefore, the original image( $I$ ) is represented by a set of subband at several scales and it is a multi-scale representation of the original image  $I$  at a depth of  $d$ .

$$\{L_d, D_{ni} \mid n=1 \dots d, i=1, 2, 3\}
 \tag{6}$$

This decomposition is called discrete wavelet decomposition or pyramid wavelet decomposition. Every decomposed subband contains information of specific scale and direction, and spatial information is retained in the subband<sup>[6][7]</sup>.

### 2.2 Wavelet Decomposition for Plate Region Extraction

DWT block diagram for plate region extraction is shown in Fig. 2. The vehicle image is decomposed by DWT at each step and decomposed subband is used selectively. We use the energy distribution of HFS for the plate region extraction.

Energy magnitude of HFS varies depending on wavelet filters, which are used for DWT. The energy of each HFS is given by

$$E_{ni} = \int (D_{ni}(b))^2 db
 \tag{7}$$

Wavelet energy  $\{E_{ni}\}_{n=1d, i=1,2,3}$  represents the energy distribution of each HFS. Table 1 shows energy distribution of a vehicle plate region according to the wavelet filter type. If the energy of HFS is too high, it is difficult to separate the plate region because other regions can also have high energy. This can lead to falsely extracting a region that has a similar energy distribution as the plate region. On the contrary, if the energy of HFS is too low, it is difficult to get high frequency component from the plate region and can easily fail to extract the plate region. Table 2 shows energy magnitude of the H-R-H region and the plate region in a vehicle image. From Table 2, we know that more than about 80% of energy of a vehicle image is converged to the H-R-H region and the plate region. Therefore, if we select an appropriate wavelet filter and use energy concentration property of the H-R-H region and the plate region, we may extract the plate region more easily. In this paper, we used biorthogonal spline 3.7 wavelet for the plate region restriction and used Haar wavelet for region extraction empirically.

Table 1. HFS energy according to wavelet filter types

	haar	db8	db16	spline2.2	spline3.7
E11	39,697	20,108	19,118	14,994	11,657
E12	25,401	13,106	12,450	12,007	9,126
E13	2,414	1,207	1,275	827	449

Table 2. The energy distribution property of H-R-H and plate region

	haar	db8	db16	spline2.2	spline3.7
Horiz.	31,858	16,566	15,492	12,132	945
Vert.	16,178	9,154	8,667	8,742	700
Diag.	1,994	960	980	68	35



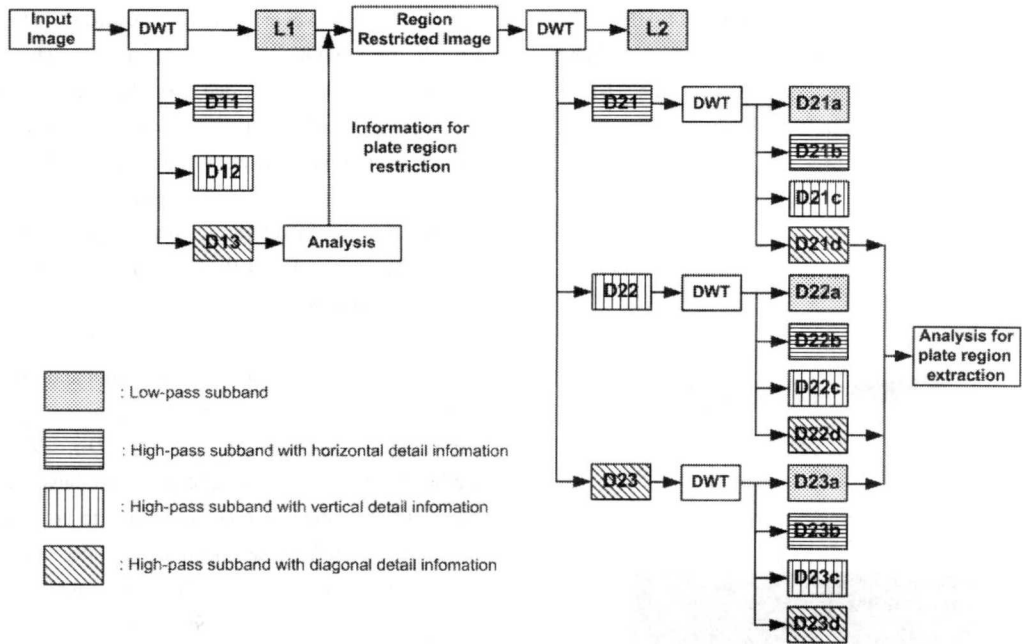


Fig. 2 DWT block diagram for the plate region extraction

### III. Plate Region Extraction

#### 3.1 Image Acquisition and Property of the Plate Region

A Vehicle Image Acquisition System (VIAS) is being installed on a highway, which is shown in Fig. 3(a), for traffic control and speeding vehicles regulation etc., and consists of Loop Detect System, CCD Camera and Control Box. The image acquisition occurs while the vehicle is passing through the Loop Detector. The vehicle's speed is inputted by the Loop Detector and measured by the Control Box. A CCD Camera mounted on the framework acquires the image.

The acquired vehicle plate region by VIAS has the following peculiar characteristics: (1) Continuous characters of regular size exist and color difference between character and plate background cause variation of intensity; (2) Edge information is concentrated in each direction of the H-R-H region and the license plate region than any other region in a vehicle image; (3) Generally, the plate region is located on the bottom of the H-R-H region that has most of the edge information for each

direction. Fig. 3 shows the acquired vehicle image by VIAS.

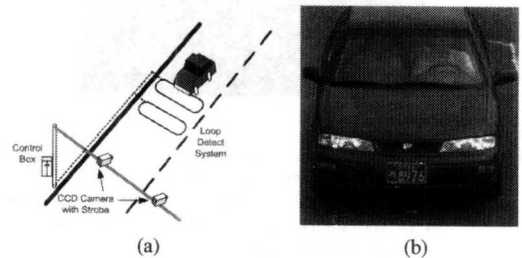


Fig. 3 (a) Vehicle Image Acquisition System (VIAS), and (b) the acquired vehicle image by VIAS.

#### 3.2 Plate Region Extraction

By decomposing an image using DWT, the energy that each pixel has in its spatial domain is decomposed into each frequency component in transform domain. First, we need to decompose the vehicle image showed in Fig. 3(b) using spline wavelet. Then, the extraction region is restricted under the H-R-H region for exact region extraction using horizontal projection. The horizontal projection of HFS is given by

$$P_h^i(x) = \sum_y D_{hi}(x, y) \tag{8}$$

where  $x, y$  are coefficient coordinates of HFS. The HFS for horizontal projection uses  $D_{13}$  subband that effectively represents the edge of the H-R-H region in a vehicle image. Fig. 4 shows the results.

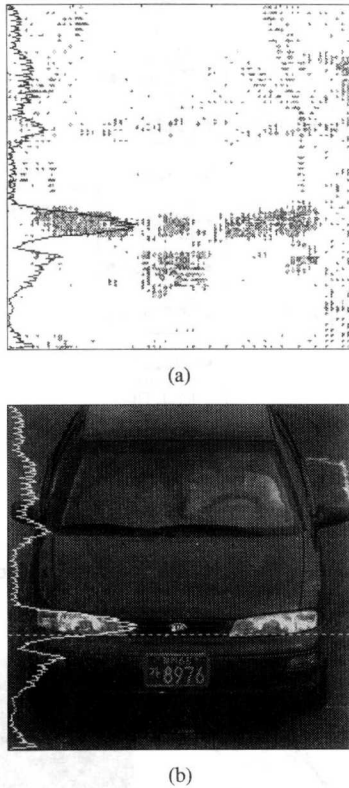


Fig. 4 The results of horizontal projection: (a) represents the distribution of D13 coefficients and  $Ph_3(y)$ , and (b) is result of mapping  $Ph_3(y)$  into D13 LFS. The dotted line in figure (b) is represents  $y'$  information for region restriction.

As shown in Fig. 4,  $P_h^3(y)$  has a maximum peak in the H-R-H region of a vehicle image. Therefore, we can use  $y$  that has a maximum value of  $\{P_h^3(y)\}_{max}$  from  $P_h^3(y)$  to restrict the extraction region under the H-R-H region.  $y$  in

$\{P_h^3(y)\}_{max}$ , however, varies according to the vehicle type within the H-R-H region. Therefore, as shown in Fig. 4(b), we can determine position  $y' = y - j$  which is moving position  $y$  downward by  $j$  as region restriction information. By doing this, we can extract the plate region more accurately by excluding the high frequency component from the H-R-H region. We determined  $j$  as 20 empirically.

For the plate region extraction, we performed wavelet decomposition over  $L_1$  subband that is restricted under the H-R-H region by  $y'$ .  $L_1$  subband is decomposed into  $L_2, D_{21}, D_{22}, D_{23}$  subbands.  $D_{21}, D_{22}, D_{23}$  subbands can have similar edges to the plate region according to a vehicles' structure. Therefore, we need to exclude horizontal and vertical edges in  $D_{21}, D_{22}, D_{23}$  subbands, and extract diagonal direction edges that represents the plate region properly. For this, as shown in Fig. 2, we need to decompose  $D_{21}, D_{22}, D_{23}$  subbands using the Haar wavelet, and select  $D_{21d}$  of  $D_{21}, D_{22d}$  of  $D_{22}$ , and  $D_{23a}$  of  $D_{23}$  HFS as the subbands for region extraction. We need to calculate the average value  $A_d = (D_{21d} + D_{22d} + D_{23a})/3$  of each subband to make the plate region prominent. Fig. 5 shows the three subbands and the average value  $A_d$ .

As shown in Fig. 5(d), the average value  $A_d$  of the plate region for each subband is represented in peak shape with certain magnitude. However,  $A_d$  region can include a whole plate region perfectly or just part of the plate region. Therefore, it is necessary to expand the region of  $A_d$  to a certain size, so that  $A_d$  can include the whole plate region. As shown in (a) of Fig. 6, to expand the region of  $A_d$ , we need to get the correlation coefficients of  $A_d, D_{21d}, D_{22d}$  and  $D_{23a}$ , and add the most

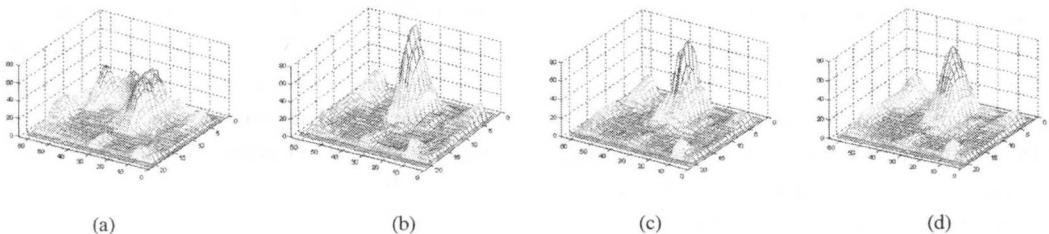


Fig. 5 Each subband and average for region extraction: (a), (b), (c) are D21, D22, D23 subband respectively, and (d) average value  $A_d$  of D21, D22, D23 subband.

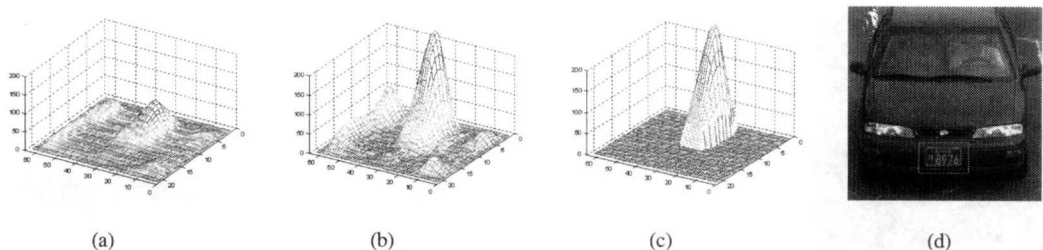


Fig. 6 (a) represents plate region  $S_R$  which is expanded by  $A_d$  and correlation coefficient of subband  $D_{21d}, D_{22d}, D_{23a}$ , and (b) contrast enhanced  $CE$  of  $S_R$ . (c) result of reference value and cardinal points search. (d) represents the result of mapping coordinates of plate region determined in (c) into vehicle image

significant correlation coefficients to  $A_d$  as weight value. The correlation coefficient  $R_{eu}$  of two 2-dimensional spaces is given by

$$R_{eu} = \frac{\sum_x \sum_y (e_{xy} - \bar{e})(u_{xy} - \bar{u})}{\sqrt{(\sum_x \sum_y (e_{xy} - \bar{e})^2)(\sum_x \sum_y (u_{xy} - \bar{u})^2)}} \quad (9)$$

where  $e=A_d, u=D_{21d}, D_{22d}, D_{23a}$ , and  $\bar{e}, \bar{u}$  are average of  $e, u$ .  $x, y$  the coordinates of  $e, u$ . The contrast of the plate region and the other region can be enhanced by Eq. (10) for the expanded plate region  $S_R=(A_d+\{R_{eu}\}_{max})/2$ .  $\{S_R\}_{max}, \{S_R\}_{min}$  in Eq. (10) denotes the maximum and minimum values in the expanded plate region  $S_R$ , and  $x, y$  are coordinates.  $z$  is a scale constant for enhancement.

$$CE(x, y) = \frac{z(S_R(x, y) - \{S_R\}_{min})}{\{S_R\}_{max} - \{S_R\}_{min}} \quad (10)$$

The contrast enhanced plate region is distinguished from the other region such as in Fig. 6(b).

Lastly, the average of  $CE$  is determined as the reference value  $T_{CE}$ , and the coordinate of the plate region is determined by selecting the inflection point or the point which has a smaller value than  $T_{CE}$  among the cardinal points(N, S, E, W) at the coordinate that has maximum  $CE$  value. Therefore, the coordinates  $CR_{N,S,E,W}$  of the plate region satisfy following two conditions.

$$\begin{aligned} CR_{N,S,E,W}(x, y) &= CE(x, y) < T_{CE} \text{ or} \\ CR_N(x, y) &= CE(x, y+1) < CE(x, y) < CE(x, y-1), \\ CR_S(x, y) &= CE(x, y-1) < CE(x, y) < CE(x, y+1), \\ CR_E(x, y) &= CE(x-1, y) < CE(x, y) < CE(x+1, y), \\ CR_W(x, y) &= CE(x+1, y) < CE(x, y) < CE(x-1, y) \end{aligned} \quad (11)$$

where the initial value of  $x, y$  are  $\{CE(x, y)\}_{max}$ .

The result from Eq. (11) is represented in Fig. 6(c), and the result of mapping coordinates into a vehicle image is represented in Fig. 6(d). As shown in Fig. 6(d), the coordinate  $CR_{N,S,E,W}$  of the extracted plate region is somewhat bigger than the actual plate region, but it includes the plate region without exception. The procedure for the plate region extraction can be summarized as following.

**Procedure:** Plate region extraction using wavelet decomposition

- [Step 1] Perform wavelet decomposition for vehicle image.
- [Step 2] Project HFS horizontally and restrict region to under H-R-H by moving position  $y$  of  $\{P_h^3(y)\}_{max}$  to downward by  $-j$ .
- [Step 3] Perform wavelet decomposition for subband  $L_1$
- [Step 4] Perform wavelet decomposition for subband  $D_{21}, D_{22}, D_{23}$ .
- [Step 5] Use decomposed  $D_{21}, D_{22}, D_{23}$  subband for region extraction, average subband and get  $A_d$ .
- [Step 6] To get the expanded region  $S_R$  of  $A_d$ , calculate correlation coefficient among  $A_d, D_{21d}, D_{22d}, D_{23a}$ .
- [Step 7] Enhance contrast of region  $S_R$ , search the cardinal points, choose plate region coordinate between inflection point and the point which has a smaller value than  $T_{CE}$ .

#### IV. Experimental Results

To evaluate the performance of the proposed method, the experiment was performed on a Pentium Pro PC using MATLAB software. Vehicle



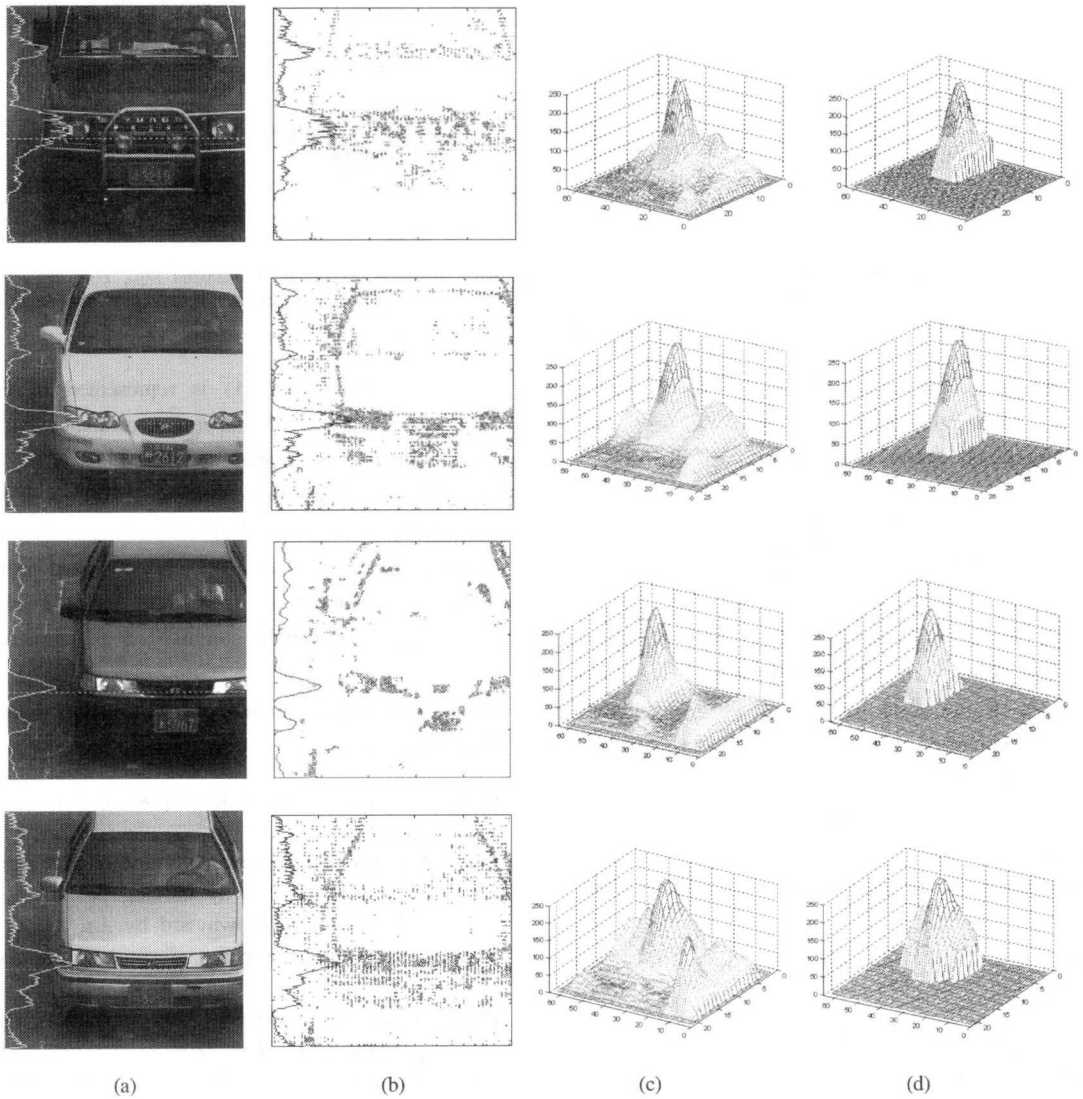


Fig. 7 Vehicle image acquisition and plate region extraction: (a) is the result of horizontal projection to restrict extraction region to bottom of H-R-H, (b) shows distribution of D13, (c) is the contrast enhanced and subband averaged image for plate region extraction, (d) is shows the plate which was extracted by cardinal points search.

image is 1024x1024 resolution gray level image and was acquired on the highway, as shown in Fig. 3(a). Down-sampled image to 512x512 was used instead of using the original image. Fig. 7 shows the results of the plate region extraction for various types of vehicle.

As shown in Fig. 7 and Fig. 8, the plate region extraction was successful for vehicles of normal condition. Although we succeeded restricting the extraction region to the bottom of the H-R-H, the extracted plate region of the last car is bigger than

the others due to the deformation of the plate.

For the performance comparison, we also experimented with 80 vehicle images using Feature Based, Gray-level Based and Color Based methods. As shown in Table 3, the proposed method performed better than existing methods and could solve the problems of those methods which has performance variation and low accuracy depending on the vehicle structure, surrounding and color of the vehicle.



Fig. 8 Represents the result of mapping coordinates of plate region determined in (d) of Fig. 7 into vehicle image

Table 3. Comparison results: Proposed method shows highest accuracy

	Feature Based	Intensity Based	Color Based	Proposed Method
Extraction	63/80	66/80	71/80	78/80
Rate (%)	78.7	82.5	88.7	97.5

### V. Conclusions

In this paper, we propose a new method of plate region extraction. We applied the edge property of a vehicle plate region to HFS of wavelet-decomposed image. We verified the proposed method with various vehicle images and compared the performance to existing methods. In the result, we could avoid the problems of other methods, and showed a 97.5% accuracy. Our proposed method can be applied to the Automatic Plate Number Recognition System and assist in the extraction of the region of interest.

We will continue our experimentation with more test images and the accuracy of the character recognition for the extracted plate region.

### References

- [1] Lu, J., Rechterik, M., and Yang, S., "Analysis of AVI technology applications to toll collection services," Transportation Research Record 1588, pp.1825, 1997.
- [2] Mei Yu and Y. D. Kim, An approach to Korean license plate recognition based on vertical edge matching, Systems, Man and Cybernetics, 2000 IEEE International Conference, vol.4, pp.2975-2980, 2000.
- [3] E. R. Lee, P. K. Kim, and H. J. Kim, Automatic recognition of a car license plate using color image processing, IEEE International Conference on Image Processing, vol. 2, pp.301-305, 1994.
- [4] S. K. Kim, D. W. Kim, and H. J. Kim, A recognition of vehicle license plate using a genetic algorithm based segmentation, IEEE International Conference on Image Processing, vol. 4, pp.661-664, 1996.
- [5] T. Shioyama, H. Wu, and T. Nojima, Recognition algorithm based on wavelet transform for



handprinted Chinese characters, 14th International Conference on Pattern Recognition, vol. 1, pp.229-232, 1998.8.

- [6] S. Mallat, A Theory for multiresolution signal decomposition: the wavelet representation, IEEE Trans. Pattern Analysis and Machine Intelligence, vol. 11, pp.674-693, 1989.
- [7] Scheunders P., Livens S., Van de Wouwer G., Vautrot P., and Van Dyck D., Wavelet-based texture analysis, International Journal on Computer Science and Information Management, vol. 1, no. 2, pp. 22-34, 1998.

박 종 욱(Jong-Wook park)

정회원

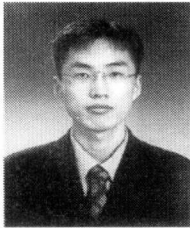


1973년 : 인하대학교  
전자공학과 학사  
1978년 : 인하대학교 대학원  
전자공학과 석사  
1985년 : 인하대학교 대학원  
전자공학과 박사

1980년~1992년 : 원광대학교 전자공학과 교수  
1992년~현재 : 인천대학교 전자공학과 교수  
<주관심 분야> 컴퓨터 비전, 인공지능, 3D 영상해석

박 성 욱(Sung-Wook Park)

정회원

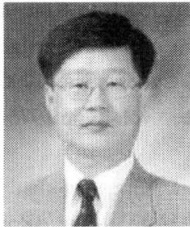


1997년 : 목원대학교  
컴퓨터공학과 학사  
1999년 : 인천대학교 대학원  
전자공학과 석사  
2000년~현재 : 인천대학교  
전자공학과 박사과정

1999년~2000년 : 한국철도기술연구원 통신연구팀  
2001년~2002년 : (주)경인기계 기술연구소  
2002년~현재 : (주)LogicMeca 멀티미디어연구소  
<주관심 분야> 컴퓨터 비전, 영상압축, 멀티미디어

황 수 철(Su-Cheol Hwang)

정회원



1986년 : 중앙대학교  
전자계산학과 학사  
1988년 : 중앙대학교 대학원  
전자계산학과 석사  
1988년 : 중앙대학교 대학원  
전자계산학과 박사

1991년 9월~현재 : 인하공업전문대학  
컴퓨터정보공학부 교수  
<주관심 분야> 지능형시스템, 전문가시스템, 인터넷  
응용